

Effect of turbulence on coagulation growth of cloud droplets

Xiang-Yu Li^{1,2,3,4,5}, A. Brandenburg^{2,4,5,6}, N. E. L. Haugen^{7,8}, B. Mehlig⁹,
I. Rogachevskii^{10,2,4}, and G. Svensson^{1,3,11}

¹Department of Meteorology and Bolin Centre for Climate Research, Stockholm University, Stockholm, Sweden

²Nordita, KTH Royal Institute of Technology and Stockholm University, 10691 Stockholm, Sweden

³Swedish e-Science Research Centre, www.e-science.se, Stockholm, Sweden

⁴Laboratory for Atmospheric and Space Physics, University of Colorado, Boulder, CO 80303, USA

⁵JILA and Department of Astrophysical and Planetary Sciences University of Colorado, Boulder, CO 80303, USA

⁶Department of Astronomy, Stockholm University, SE-10691 Stockholm, Sweden

⁷SINTEF Energy Research, 7465 Trondheim, Norway

⁸Department of Energy and Process Engineering, NTNU, 7491 Trondheim, Norway

⁹Department of Physics, Gothenburg University, 41296 Gothenburg, Sweden

¹⁰Department of Mechanical Engineering, Ben-Gurion Univ. of the Negev, P. O. Box 653, Beer-Sheva 84105, Israel

¹¹Global & Climate Dynamics, National Center for Atmospheric Research, Boulder, CO 80305, USA

Key Points:

- In high-resolution direct numerical simulations of fully-developed turbulence with a well resolved Kolmogorov scale, we determine the motion of droplets suspended in turbulence using a super-particle approach.
- We monitor the collisional aggregation of the droplets assuming unit collision efficiency, and determine the resulting time evolution of their size distribution.
- We consider turbulence-induced coagulation, neglecting gravitational settling and condensational growth. We find that the growth of cloud droplets strongly depends on the mean turbulent energy-dissipation rate per unit mass, and only weakly on the Reynolds number of the turbulent flow.

Corresponding author: Xiang-Yu Li, xiang.yu.li@su.se, Revision: 1.318

Corresponding author: Gunilla Svensson, gunilla@misu.su.se

Abstract

We investigate the effect of turbulence on the coagulation growth of μm -sized droplets by high-resolution numerical simulations with a well resolved Kolmogorov scale, assuming a collision and coalescence efficiency of unity. We approximate the droplet dynamics using a super-particle approach. The effects of gravity and condensation are not included in the simulations. We show that the time evolution of the shape of the droplet-size distribution due to turbulence-induced coagulation depends strongly on the turbulent energy-dissipation rate, but only weakly on the Reynolds number.

1 Introduction

Turbulence may enhance the collisional growth of cloud droplets [Shaw *et al.*, 1998; Shaw, 2003; Khain *et al.*, 2007, 2015; Lamb and Verlinde, 2011; Devenish *et al.*, 2012; Grabowski and Wang, 2013]. In particular, droplet inertia [Sundaram and Collins, 1997a; Falkovich *et al.*, 2002; Wilkinson *et al.*, 2006; Wang and Grabowski, 2009; Ayala *et al.*, 2008] and fluctuations of the energy-dissipation rate may enhance coagulation growth [Falkovich and Pumir, 2004; Shaw, 2003; Devenish *et al.*, 2012] by increasing the relative velocities of the colliding cloud droplets. However, those and most other earlier studies combined a parameterized coagulation kernel with direct numerical simulations (DNS) [Ayala *et al.*, 2008; Wang and Grabowski, 2009], or relied on statistical models of turbulence [Gustavsson and Mehlig, 2016] to describe turbulent coagulation.

Here we determine the droplet-size distribution directly from numerical simulations, thus avoiding the use of a parameterized kernel. Our simulations show that coagulation in fully-developed turbulence results in a wide range of droplet sizes and thus in a wide range of droplet Stokes numbers that evolve during the simulation. The Stokes number is a dimensionless measure of the effect of droplet inertia. In cloud turbulence with mean energy dissipation rate $\bar{\epsilon} \approx 0.04 \text{ m}^2\text{s}^{-3}$, the Stokes number St varies from 10^{-3} (droplet radius of about $1 \mu\text{m}$) to 10 (about $100 \mu\text{m}$) and beyond. Very small cloud droplets (for $St \ll 1$) are advected by turbulent air flow and the coagulation is caused by local turbulent shear [Saffman and Turner, 1956; Andersson *et al.*, 2007]. For larger Stokes numbers, on the other hand, inertial effects become important, that allow the droplets to detach from the flow. This may substantially increase the collision rate [Sundaram and Collins, 1997b; Falkovich *et al.*, 2002; Wilkinson *et al.*, 2006]. Here we study how changing the Reynolds number and the energy dissipation rate affects the coagulation growth of droplets in fully developed turbulence, for a wide range of Stokes numbers.

We perform high-resolution DNS of turbulence with a well resolved Kolmogorov viscous scale (our maximum Taylor-microscale Reynolds number is 158). Droplet and collision dynamics are solved together using a super-particle approach assuming unit collision efficiency. This work aims to obtain the time evolution of the size distribution of cloud droplets due to turbulent coagulation, while neglecting gravity and condensation.

2 Numerical setup

Our simulations use the PENCIL CODE. The DNS of the turbulent flow are performed for a weakly compressible gas, and we adopt a super-particle algorithm to approximate the droplet dynamics [Zsom and Dullemond, 2008; Shima *et al.*, 2009; Johansen *et al.*, 2012].

DNS of the turbulent air flow. The velocity \mathbf{u} of the turbulent air flow is determined by the Navier-Stokes equation:

$$\frac{\partial \mathbf{u}}{\partial t} + \mathbf{u} \cdot \nabla \mathbf{u} = \mathbf{f} - \rho^{-1} \nabla p + \rho^{-1} \nabla \cdot (2\nu \rho \mathbf{S}), \quad (1)$$

Table 1. Summary of the simulations.

Run	$N_p/10^6$	mesh points	$ f \cdot 10^{-2}$	L (m)	u_{rms} (m s $^{-1}$)	Re_λ	$\bar{\epsilon}$ (m 2 s $^{-3}$)	$\eta \cdot 10^{-4}$ (m)	τ_η (s)
A	8.4	256 3	2	0.125	0.17	57	0.039	4	0.016
B	67	512 3	2	0.25	0.21	94	0.04	4	0.016
C	67	512 3	2	0.50	0.27	158	0.036	4	0.017
D	67	512 3	0.72	0.44	0.13	98	0.005	7	0.044
E	67	512 3	1	0.37	0.15	97	0.01	6	0.032
F	67	512 3	1.4	0.30	0.18	94	0.02	5	0.022

Here, N_p is the number of superparticles used in the simulation, $|f|$ is the amplitude of the random forcing (see text), and L is the domain size.

where \mathbf{f} is a random forcing function [Brandenburg, 2001], ν is the kinematic viscosity of the air flow, $\mathbf{S}_{ij} = \frac{1}{2}(\partial_j u_i + \partial_i u_j) - \frac{1}{3}\delta_{ij}\nabla \cdot \mathbf{u}$ is the traceless rate-of-strain tensor, p is the gas pressure, and ρ is the gas density, which in turn obeys the continuity equation,

$$\frac{\partial \rho}{\partial t} + \nabla \cdot (\rho \mathbf{u}) = 0. \quad (2)$$

We assume that the gas is isothermal with constant sound speed c_s , so that $p = c_s^2 \rho$. The sound speed is set to 5 m s $^{-1}$, resulting in a Mach number of 0.06 when the $u_{\text{rms}} = 0.27$ m s $^{-1}$. We quantify the weak compressibility in our DNS by calculating the dimensionless number $\wp = \langle |\nabla \cdot \mathbf{u}|^2 \rangle / \langle |\nabla \times \mathbf{u}|^2 \rangle = 2 \times 10^{-4}$. Following Gustavsson and Mehlig [2016], \wp corresponds to a critical Stokes number $St = 0.018$, below which compressibility may affect the spatial distribution of the droplets. Initially, the smallest Stokes number is $St = 0.05$ in our DNS. Therefore, compressibility does not have a significant effect on the droplets. To characterize the intensity of turbulence, we use the Taylor microscale Reynolds number $\text{Re}_\lambda \equiv u_{\text{rms}}^2 \sqrt{5/(3\nu\bar{\epsilon})}$, where $u_0 = u_{\text{rms}}/\sqrt{3}$, u_{rms} is the rms turbulent velocity, and $\bar{\epsilon} = 2\nu \text{Tr} \mathbf{S}^T \mathbf{S}$ is the mean energy-dissipation rate per unit mass. The parameters of all simulations are listed in Table 1. Here $\tau_\eta = (\nu/\bar{\epsilon})^{1/2}$ is the Kolmogorov time and $\eta = (\nu^3/\bar{\epsilon})^{1/4}$ is the Kolmogorov length.

Superparticle algorithm. The equations governing the dynamics and coagulation of droplets in a turbulent flow are solved simultaneously with the Navier-Stokes equations using the PENCIL CODE. We approximate droplet dynamics and collisions using a stochastic Monte Carlo algorithm that represents a number of spherical droplets by a superparticle [Shima et al., 2009; Zsom and Dullemond, 2008; Johansen et al., 2012]. All droplets in superparticle i are assumed to have the same material density ρ_d , radius r_i , and velocity \mathbf{v}_i . Further, each superparticle is assigned a volume and thus a droplet number density, n_i . The position \mathbf{x}_i of superparticle i is determined by

$$\frac{d\mathbf{x}_i}{dt} = \mathbf{V}_i \quad (3)$$

and

$$\frac{d\mathbf{V}_i}{dt} = \frac{1}{\tau_i}(\mathbf{u} - \mathbf{V}_i). \quad (4)$$

Here, $\tau_i = 2\rho_w r_i^2 / [9\rho\nu C(\text{Re}_i)]$ is the particle response time attributed to superparticle i . The correction factor [Schiller and Naumann, 1933; Marchioli et al., 2008] $C(\text{Re}_i) = 1 + 0.15 \text{Re}_i^{0.687}$ models the effect of non-zero particle Reynolds number $\text{Re}_i = 2r_i|\mathbf{u} - \mathbf{V}_i|/\nu$. This is a widely used approximation, although it does not correctly reproduce the small- Re_i correction to Stokes formula [Veysey and Goldenfeld, 2007]. The dimensionless particle-response time is given by the Stokes number $St = \tau_i/\tau_\eta$. The effect of gravitational settling is neglected in Eq. (4). Droplet collisions are represented by collisions of superparticles [Johansen et al., 2012]. When two superparticles collide, two droplets in either of the superparticles can collide with probability $p_c = \tau_c^{-1}\Delta t$, where Δt is the integration time step. A

mean-field model is adopted for the collision time τ_c :

$$\tau_c^{-1} = \sigma_c n_j |\mathbf{V}_i - \mathbf{V}_j| E_c. \quad (5)$$

Here $\sigma_c = \pi(r_i + r_j)^2$ is the geometric collision cross section of two droplets with radii r_i and r_j . The parameter E_c is the collision efficiency [Devenish *et al.*, 2012]. It is set to unity in our simulations, and we assume that the droplets coalesce upon collision. Droplet growth by condensation is not incorporated in our model. We refer to Li *et al.* [2017] for a detailed description of our numerical setup and of the algorithm used to model coagulation.

The super-particle approach is computationally efficient [Shima *et al.*, 2009; Johansen *et al.*, 2012], but it is an approximation. How accurately it describes the actual microscopic collision dynamics depends on several factors. In the limit where the number of droplets per superparticle tends to infinity, the algorithm reduces to a full mean-field description [Zsom and Dullemond, 2008; Pruppacher *et al.*, 1998]. In the opposite limit, when the number of droplets per superparticle is small, the algorithm incorporates fluctuations in the collision processes that may be important in the dilute system we consider here [Kostinski and Shaw, 2005; Wilkinson, 2016]. But it remains an open question how accurately the algorithm describes such fluctuations [Dziekan and Pawlowska, 2017].

In our simulations we compute the droplet-size distribution function $f(r, t)$ [Shaw, 2003] at time t . Here r is the droplet radius. This distribution not only determines rain formation in clouds, but also their optical depths of the cloud [Beals *et al.*, 2015a]. As initial condition, we adopt a log-normal droplet-size distribution [Seinfeld and Pandis, 2016],

$$f(r, 0) = \frac{n_0}{\sqrt{2\pi}\sigma_{\text{ini}} r} \exp \left[-\frac{\ln^2(r/r_{\text{ini}})}{2\sigma_{\text{ini}}^2} \right]. \quad (6)$$

Here $r_{\text{ini}} = 10 \mu\text{m}$, $\sigma_{\text{ini}} = 0.2$, and $n_0 = n(t = 0)$ is the initial number density of droplets. To speed up the computation by a factor of a hundred, we adopt $n_0 = 10^{10} \text{m}^{-3}$ instead of the typical value in the atmospheric clouds, 10^8m^{-3} ; cf. Li *et al.* [2017].

3 Results and discussion

Figure 1(a) shows turbulent kinetic-energy spectra for different values of Re_λ at fixed $\bar{\epsilon} \approx 0.04 \text{m}^2\text{s}^{-3}$. Here, Re_λ is varied by changing the domain size L , which in turn changes u_{rms} . For larger Reynolds numbers the spectra extend to smaller wavenumbers. Since the energy spectrum is compensated by $\bar{\epsilon}^{-2/3} k^{5/3}$, a flat profile corresponds to Kolmogorov scaling [Pope, 2000]. For the largest Re_λ in our simulations ($\text{Re}_\lambda = 158$), the inertial range extends for about a decade in k -space. Figure 1(b) shows how the energy spectra depend on $\bar{\epsilon}$. Here we keep the values of Re_λ and ν fixed, but vary u_{rms} by changing both L and the amplitude of the forcing. Since the abscissa in the figures is normalized by $k_\eta = 2\pi/\eta$, the different spectra shown in Figure 1(b) collapse onto a single curve.

Figure 2(a) shows the droplet-size distributions obtained in our simulations for different values of Re_λ , but for the same $\bar{\epsilon}$. The Figure demonstrates that the time evolution of the size distribution depends only weakly on Re_λ when $\bar{\epsilon}$ is kept constant. This is consistent with the notion that the coagulation growth is mainly dominated by the Kolmogorov scales [Devenish *et al.*, 2012]. The maximum Reynolds number in our DNS is $\text{Re}_\lambda \approx 158$. This value is still two orders of magnitude smaller than the typical value in atmospheric clouds [Grabowski and Wang, 2013]. It cannot be ruled out that there may be a stronger Reynolds-number effect on the coagulation growth at higher Reynolds numbers [Shaw, 2003; Ireland *et al.*, 2016; Onishi and Seifert, 2016]. In the simulations of Onishi and Seifert [2016], the largest value of Re_λ was 333, which is twice as large as our largest value. They showed that the turbulence enhancement factor weakly depends on Re_λ when the mean radius of the initial distribution is $10 \mu\text{m}$. This is consistent with our results.

Figure 2(b) shows how the evolution of the droplet-size distribution depends on $\bar{\epsilon}$, for a fixed Re_λ . We see that especially the tails of the size distributions depend strongly on $\bar{\epsilon}$:

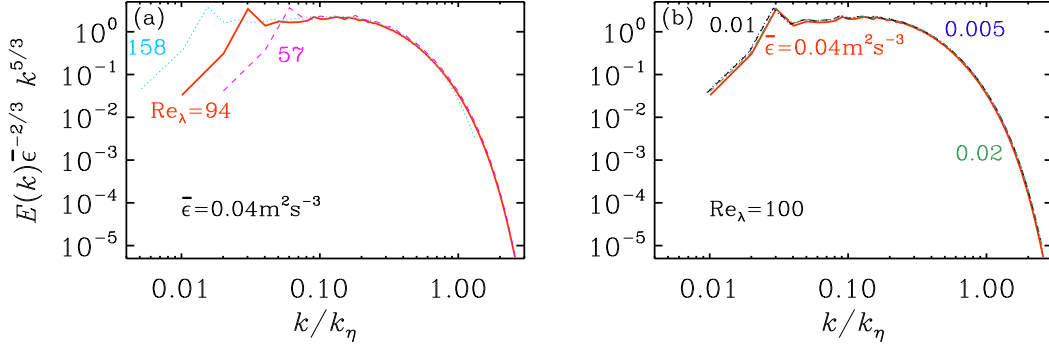


Figure 1. Turbulent kinetic-energy spectra for (a) different $Re_\lambda = 57$ (magenta dashed line), 94 (red solid line), and 158 (cyan dotted line) at fixed $\bar{\epsilon} = 0.04 \text{ m}^2 \text{ s}^{-3}$ (see Runs A, B, and C in Table 1 for details) and for (b) different $\bar{\epsilon} = 0.005 \text{ m}^2 \text{ s}^{-3}$ (blue dotted line), 0.01 (black dashed line), 0.02 (green dash-dotted line) and 0.04 (red solid line) at fixed $Re_\lambda = 100$ (see Runs B, D, E, and F in Table 1 for details).

the larger $\bar{\epsilon}$, the wider are the tails. The tails in the droplet-size distribution lead to a broad distribution of Stokes numbers. Also, since $St = \tau_i/\tau_\eta \propto \bar{\epsilon}^{1/2}$, the St -distribution shifts to large Stokes numbers as $\bar{\epsilon}$ increases.

We now show that the $\bar{\epsilon}$ -dependence of the size distribution is due to the sensitive dependence of the collision rate upon this parameter. Figure 3 shows how the mean collision rate \bar{R}_c changes as a function of time. This rate, which depends implicitly on $\bar{\epsilon}$, is defined as

$$\bar{R}_c = 2\pi n_0 (2r)^2 |\bar{v}_r|, \quad (7)$$

where v_r is the relative radial velocity of approaching droplets. This expression is written for identical droplets with radius r . In bidisperse suspensions with droplets of two different radii r_i and r_j , $2r$ is replaced by $r_i + r_j$. Collisions of small droplets advected by turbulence are due to local turbulent shear, provided that droplet inertia is negligible. *Saffman and Turner* [1956] proposed an expression for the resulting collision rate:

$$R_c^{\text{S.T.}} = \frac{C n_0 (2r)^3}{\tau_\eta}. \quad (8)$$

Saffman and Turner [1956] quote the value $C = \sqrt{8\pi/15}$ for the prefactor, but this is just an approximation, even at $St = 0$ [Voßkuhle *et al.*, 2014]. It turns out that the Saffman-Turner estimate is an upper bound, because it counts recollisions that must not be counted when the droplets coalesce upon collision, as in our simulations. DNS of small droplets in turbulence also count recollisions (no coalescence) and yield a value of C in good agreement with the Saffman-Turner estimate [Voßkuhle *et al.*, 2014], in the limit of $St \rightarrow 0$.

In Figure 3(a) we normalized the mean collision rate by dividing with the Saffman-Turner expression (8) for the collision rate, averaging $(2r)^3 = (r_i + r_j)^3$ over the initial size distribution. Initially the collision rate is of the same order as predicted by Eq. (8), but in our simulations the coefficient C depends on $\bar{\epsilon}$. It ranges from $C \approx 1.57$ at $\bar{\epsilon} = 0.005 \text{ m}^2 \text{ s}^{-3}$ to $C \approx 2.26$ at $\bar{\epsilon} = 0.04 \text{ m}^2 \text{ s}^{-3}$. All values are somewhat larger than the Saffman-Turner prediction. This appears at variance with the expectation that the Saffman-Turner collision rate should be an upper bound for advected droplets. However, in our simulations the mean Stokes number ranges from $St = 0.05$ for $\bar{\epsilon} = 0.005 \text{ m}^2 \text{ s}^{-3}$ to $St = 0.14$ for $\bar{\epsilon} = 0.04 \text{ m}^2 \text{ s}^{-3}$. From Figure 1 of Voßkuhle *et al.* [2014] we infer that $C = 1.9$ for $St = 0.05$, in reasonable agreement with our simulation results. However, their $C = 5$ for $St = 0.14$, which is about twice as large as our value ($C \approx 2.26$). This overestimation of C at $St = 0.14$ could

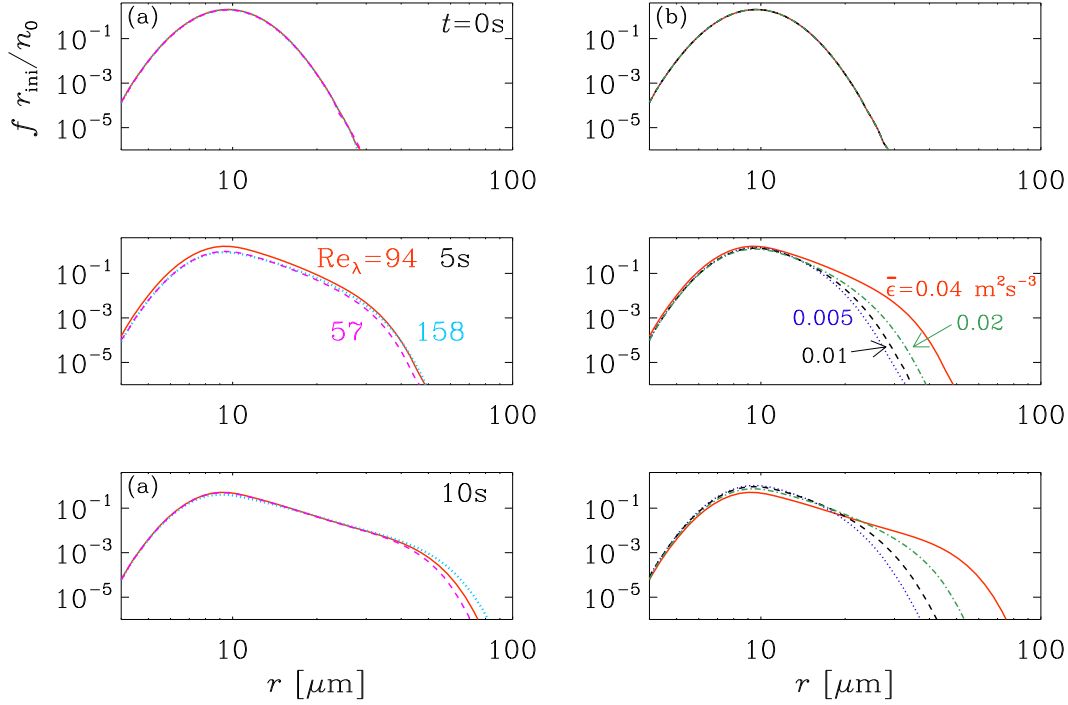


Figure 2. Droplet-size distribution for the same simulations as in Figure 1. Panel (a): different Re_λ at fixed $\bar{\epsilon}$. Panel (b): different $\bar{\epsilon}$ at fixed Re_λ .

be due to their recollisions. We conclude that the collision rate scales initially as predicted by the Saffman-Turner theory, $R_c \sim \sqrt{\bar{\epsilon}}$, with small corrections due to particle inertia. At later times these corrections become larger. In recent years, several works have indicated that the Saffman-Turner model underestimates the collision rate at larger Stokes numbers when the effect of droplet inertia becomes important, so that the droplets can detach from the flow. Model calculations show that this can substantially enhance the collision rate. Two mechanisms have been proposed.

First, droplet inertia causes identical droplets to cluster spatially [Maxey, 1987; Elperin *et al.*, 1996, 2002; Reade and Collins, 2000; Kostinski and Shaw, 2001; Bec, 2003; Duncan *et al.*, 2005; Elperin *et al.*, 2013; Gustavsson and Mehlig, 2016]. At small spatial scales the clustering of identical droplets is fractal. This enhances the collision rate of small droplets [Gustavsson *et al.*, 2008a]: $R_c = C n_0 (2r)^3 \tau_\eta^{-1} g(2r)$. Here $g(2r)$ is the pair correlation function measuring the degree of fractal clustering of identical droplets: $g(2r)$ diverges $\sim r^{-\xi}$ as $r \rightarrow 0$ with $\xi > 0$. The exponent ξ has been computed in DNS and model calculations [Gustavsson and Mehlig, 2016]. It has a weak dependence on $\bar{\epsilon}$. Our numerical data is not precise enough to attempt a quantitative comparison with this theory. But more importantly, coagulation leads to a distribution of droplet sizes. Droplets of different sizes cluster onto different fractal attractors. This may reduce the effect of spatial clustering on the collision rate [Chun *et al.*, 2005; Bec *et al.*, 2005; Meibohm *et al.*, 2017].

Second, singularities in the droplet dynamics (so-called caustics) give rise to multi-valued droplet velocities, resulting in large velocity differences between nearby droplets [Sundaram and Collins, 1997b; Falkovich *et al.*, 2002; Wilkinson *et al.*, 2006; Falkovich and Pumir, 2007; Gustavsson and Mehlig, 2014; Voßkuhle *et al.*, 2014]. Most model calculations were performed for identical droplets. They indicate that the enhancement of the collision rate due to multi-valued droplet velocities dominates for Stokes numbers larger than unity [Voßkuhle *et al.*,

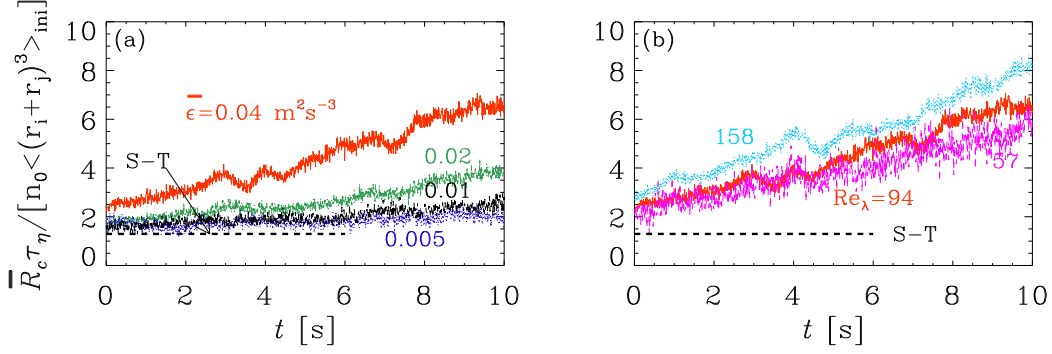


Figure 3. Mean coagulation rate for same simulations as in Figure 1. Panel (a): different $\bar{\epsilon}$ at fixed Re_λ . Panel (b): different Re_λ at fixed $\bar{\epsilon}$. In both panels the data are normalized by dividing by $n_0 \langle (r_i + r_j)^3 \rangle_{ini} / \tau_\eta$.

2014]. In this case, a Kolmogorov-scaling argument suggests [Mehlig *et al.*, 2007; Gustavsson *et al.*, 2008b] that $R_c \sim n_0 r^2 u_K \sqrt{St} \propto \bar{\epsilon}^{1/2}$; the \sqrt{St} -dependence was first suggested by Völk *et al.* [1980], using a different argument. This expression has the same $\bar{\epsilon}$ -dependence as Eq. (8). We note, however, that the Kolmogorov-scaling argument leading to this \sqrt{St} -dependence rests on the assumption that there is a well developed inertial range ($Re_\lambda \rightarrow \infty$). This assumption is not fulfilled in our simulations. Moreover, at later times we expect that collisions between droplets of different sizes make an important contribution [Meibohm *et al.*, 2017]. Scaling theory [Mehlig *et al.*, 2007] suggests that the $\bar{\epsilon}$ -scaling remains the same in the limit of $Re_\lambda \rightarrow \infty$. But, again, this limit is not realized in our simulations. Also, any theory for the collision rate in bidisperse suspensions must be averaged over the distribution of particle sizes and their velocities to allow comparison with Figure 3(a). This may introduce additional $\bar{\epsilon}$ -dependencies. It is therefore plausible that the small- St scaling, $R_c \sim \sqrt{\bar{\epsilon}}$, breaks down in our simulations at larger Stokes numbers, indicating that the increase in the mean collision rate is an inertial effect. Moreover, since the Stokes numbers are larger for larger values of $\bar{\epsilon}$, we expect the inertial additive corrections to the collision rate (due to clustering and increased relative particle velocities) to be larger at larger $\bar{\epsilon}$. This is consistent with Figure 3(a). In conclusion, the mean collision rate depends strongly on $\bar{\epsilon}$ (Figure 3(a)), as do the size distributions shown in Figure 2(b).

Figure 3(b) shows that the mean collision rate depends only weakly on the Reynolds number. It demonstrates that the collision rate is somewhat larger for larger Reynolds numbers. This is consistent with the notion that particle pairs exploring the inertial range collide at larger relative velocities when the inertial range is larger [Gustavsson *et al.*, 2008b]. But, as pointed out above, the inertial range in our simulations is too small for this mechanism to have a substantial effect.

In cloud-droplet formation, gravitational settling is significant [Grabowski and Wang, 2013], which is neglected here. The interplay between turbulence and settling gives rise to new mechanisms [Eidelman *et al.*, 2010; Bec *et al.*, 2014; Gustavsson *et al.*, 2014] that are not discussed here.

Kostinski and Shaw [2005] proposed that Poisson fluctuations of the collision times of settling droplets leads to a broad distribution of growth times that could potentially explain the rapid onset of rain formation. This question is further discussed by Wilkinson [2016]. Whether or not this mechanism can explain the fast warm rain formation is a question for future research.

Condensation of water vapor on droplets is also neglected here. This is important in the size range of $1 - 10 \mu\text{m}$ [Lamb and Verlinde, 2011]. Several recent works suggest that supersaturation fluctuations due to turbulence [Sardina *et al.*, 2015; Chandrakar *et al.*, 2016] and entrainment [Grabowski and Wang, 2013; Beals *et al.*, 2015b] may broaden the droplet-size distribution.

4 Conclusions

In the present study we addressed the problem of turbulence effects on coagulation growth of cloud droplets. We investigated this effect using a super-particle approximation for the droplet dynamics in combination with high-resolution DNS of fully-developed turbulence. We found that the droplet-size distribution depends sensitively on the mean energy-dissipation rate $\bar{\epsilon}$ at fixed Re_λ , which we related to the $\bar{\epsilon}$ -dependence of the mean collision rate. We found that this rate increases as $\bar{\epsilon}^{1/2}$ (except for the largest values of $\bar{\epsilon}$ simulated). This is consistent with the Saffman-Turner collision model and its extensions. A more detailed comparison with these calculations is not possible at this point, because there is no definite prediction for the prefactors in general. Also, the model calculations neglect fluctuations of local energy dissipation rates. Since these may substantially affect the coagulation process, it is necessary to study their role using numerical simulations. We plan to address this question in a future study. Finally, it must be borne in mind that the super-particle approach approximates local collision processes. It remains to be seen where this matters. Preliminary results indicate that this approach can at least qualitatively describe the effect of fluctuations in local collision processes [Dziekan and Pawłowska, 2017], but further studies are needed, especially for dilute systems and in the presence of turbulence.

Acknowledgments

We thank Akshay Bhatnagar and Gregory Falkovich for stimulating discussions. This work was supported through the FRINATEK grant 231444 under the Research Council of Norway, SeRC, the Swedish Research Council grants 2012-5797 and 2013-03992, and the grant “Bottlenecks for particle growth in turbulent aerosols” from the Knut and Alice Wallenberg Foundation, Dnr. KAW 2014.0048. Gunilla Svensson also thanks the Wenner-Gren Foundation for their support. The simulations were performed using resources provided by the Swedish National Infrastructure for Computing (SNIC) at the Royal Institute of Technology in Stockholm and Chalmers Centre for Computational Science and Engineering (C3SE). This work also benefited from computer resources made available through the Norwegian NOTUR program, under award NN9405K. The source code used for the simulations of this study, the PENCIL CODE, is freely available on <https://github.com/pencil-code/>. The input files as well as some of the output files of the simulations listed in Table 1 are available under http://www.nordita.org/~brandenb/projects/collision_turbulence/.

References

- Andersson, B., K. Gustavsson, B. Mehlig, and M. Wilkinson (2007), Advective collisions, *Europhys. Lett.*, *80*(6), 69,001.
- Ayala, O., B. Rosa, and L.-P. Wang (2008), Effects of turbulence on the geometric collision rate of sedimenting droplets. part 2. theory and parameterization, *New J. Phys.*, *10*(9), 099,802.
- Beals, M. J., J. P. Fugal, R. A. Shaw, J. Lu, S. M. Spuler, and J. L. Stith (2015a), Holographic measurements of inhomogeneous cloud mixing at the centimeter scale, *Science*, *350*(6256), 87–90.
- Beals, M. J., J. P. Fugal, R. A. Shaw, J. Lu, S. M. Spuler, and J. L. Stith (2015b), Holographic measurements of inhomogeneous cloud mixing at the centimeter scale, *Science*, *350*(6256), 87–90.

- Bec, J. (2003), Fractal clustering of inertial particles in random flows, *Phys. Fluids*, *15*, 81–84.
- Bec, J., A. Celani, M. Cencini, and S. Musacchio (2005), Clustering and collisions in random flows, *Phys. Fluids*, *17*, 073301.
- Bec, J., H. Homann, and S. Sankar Ray (2014), Gravity-driven enhancement of heavy particle clustering in turbulent flow, *Phys. Rev. Lett.*, *112*, 184501.
- Brandenburg, A. (2001), The inverse cascade and nonlinear alpha-effect in simulations of isotropic helical hydromagnetic turbulence, *Astrophys. J.*, *550*(2), 824.
- Chandrakar, K. K., W. Cantrell, K. Chang, D. Ciochetto, D. Niedermeier, M. Ovchinnikov, R. A. Shaw, and F. Yang (2016), Aerosol indirect effect from turbulence-induced broadening of cloud-droplet size distributions, *Proc. Nat. Acad. Sci.*, *113*(50), 14,243–14,248.
- Chun, J., D. L. Koch, S. L. Rani, A. Ahluwalia, and L. R. Collins (2005), Clustering of aerosol particles in isotropic turbulence, *J. Fluid Mech.*, *536*, 219–251.
- Devenish, B., P. Bartello, J.-L. Brenguier, L. Collins, W. Grabowski, R. IJzermans, S. Malinowski, M. Reeks, J. Vassilicos, L.-P. Wang, et al. (2012), Droplet growth in warm turbulent clouds, *Quart. J. Roy. Meteorol. Soc.*, *138*(667), 1401–1429.
- Duncan, K., B. Mehlig, S. Östlund, and M. Wilkinson (2005), Clustering in mixing flows, *Phys. Rev. Lett.*, *95*, 240602.
- Dziekan, P., and H. Pawłowska (2017), Stochastic coalescence in Lagrangian cloud microphysics, *Atmosph. Chemistry and Physics*, *2017*, 1–18.
- Eidelman, A., T. Elperin, N. Kleeorin, B. Melnik, and I. Rogachevskii (2010), Tangling clustering of inertial particles in stably stratified turbulence, *Phys. Rev. E*, *81*(5), 056313.
- Elperin, T., N. Kleeorin, and I. Rogachevskii (1996), Self-excitation of fluctuations of inertial particle concentration in turbulent fluid flow, *Phys. Rev. Lett.*, *77*, 5373–5376.
- Elperin, T., N. Kleeorin, V. S. L’vov, I. Rogachevskii, and D. Sokoloff (2002), Clustering instability of the spatial distribution of inertial particles in turbulent flows, *Phys. Rev. E*, *66*, 036,302.
- Elperin, T., N. Kleeorin, M. Liberman, and I. Rogachevskii (2013), Tangling clustering instability for small particles in temperature stratified turbulence, *Phys. Fluids*, *25*(8), 085,104.
- Falkovich, G., and A. Pumir (2004), Intermittent distribution of heavy particles in a turbulent flow, *Phys. Fluids*, *16*(7), L47–L50.
- Falkovich, G., and A. Pumir (2007), Sling effect in collisions of water droplets in turbulent clouds, *J. Atmosph. Sci.*, *64*(12), 4497–4505.
- Falkovich, G., A. Fouxon, and M. Stepanov (2002), Acceleration of rain initiation by cloud turbulence, *Nature*, *419*(6903), 151–154.
- Grabowski, W. W., and L.-P. Wang (2013), Growth of cloud droplets in a turbulent environment, *Annu. Rev. Fluid Mech.*, *45*(1), 293–324.
- Gustavsson, K., and B. Mehlig (2014), Relative velocities of inertial particles in turbulent aerosols, *J. Turbulence*, *15*(1), 34–69.
- Gustavsson, K., and B. Mehlig (2016), Statistical models for spatial patterns of heavy particles in turbulence, *Advances in Physics*, *65*(1), 1–57.
- Gustavsson, K., B. Mehlig, and M. Wilkinson (2008a), Collisions of particles advected in random flows, *New J. Phys.*, *10*(7), 075,014.
- Gustavsson, K., B. Mehlig, M. Wilkinson, and V. Uski (2008b), Variable-range projection model for turbulence-driven collisions, *Phys. Rev. Lett.*, *101*, 174503.
- Gustavsson, K., S. Vajedi, and B. Mehlig (2014), Clustering of particles falling in a turbulent flow, *Phys. Rev. Lett.*, *112*, 214,501.
- Ireland, P. J., A. D. Bragg, and L. R. Collins (2016), The effect of reynolds number on inertial particle dynamics in isotropic turbulence. part 1. simulations without gravitational effects, *J. Fluid Mech.*, *796*, 617–658.
- Johansen, A., A. N. Youdin, and Y. Lithwick (2012), Adding particle collisions to the formation of asteroids and Kuiper belt objects via streaming instabilities, *Astron. Astroph.*, *537*, A125.

- Khain, A., M. Pinsky, T. Elperin, N. Kleeorin, I. Rogachevskii, and A. Kostinski (2007), Critical comments to results of investigations of drop collisions in turbulent clouds, *Atmosph. Res.*, 86(1), 1 – 20.
- Khain, A., K. Beheng, A. Heymsfield, A. Korolev, S. Krichak, Z. Levin, M. Pinsky, V. Phillips, T. Prabhakaran, A. Teller, et al. (2015), Representation of microphysical processes in cloud-resolving models: Spectral (bin) microphysics versus bulk parameterization, *Rev. Geophys.*, 53(2), 247–322.
- Kostinski, A. B., and R. A. Shaw (2001), Scale-dependent droplet clustering in turbulent clouds, *J. Fluid Mech.*, 434, 389–398.
- Kostinski, A. B., and R. A. Shaw (2005), Fluctuations and luck in droplet growth by coalescence, *Bull. Am. Met. Soc.*, 86, 235–244.
- Lamb, D., and J. Verlinde (2011), *Physics and Chemistry of Clouds*, Cambridge, England, Cambridge Univ. Press.
- Li, X.-Y., A. Brandenburg, N. E. L. Haugen, and G. Svensson (2017), Eulerian and Lagrangian approaches to multidimensional condensation and collection, *J. Advances Model. Earth Systems*, 9, 1116–1137.
- Marchioli, C., A. Soldati, J. Kuerten, B. Arcen, A. Taniere, G. Goldensoph, K. Squires, M. Cargnelutti, and L. Portela (2008), Statistics of particle dispersion in direct numerical simulations of wall-bounded turbulence: Results of an international collaborative benchmark test, *Intern. J. Multiphase Flow*, 34(9), 879–893.
- Maxey, M. (1987), The gravitational settling of aerosol particles in homogeneous turbulence and random flow fields, *J. Fluid Mech.*, 174, 441–465.
- Mehlig, B., M. Wilkinson, and V. Uski (2007), Colliding particles in highly turbulent flows, *Phys. Fluids*, 19, 098107.
- Meibohm, J., L. Pistone, K. Gustavsson, and B. Mehlig (2017), Relative velocities in bidisperse turbulent suspensions, *e-preprint*, [arXiv:1703.01669](https://arxiv.org/abs/1703.01669).
- Onishi, R., and A. Seifert (2016), Reynolds-number dependence of turbulence enhancement on collision growth, *Atmosph. Chemistry and Physics*, 16(19), 12,441–12,455.
- Pope, S. (2000), *Turbulent Flows*, Cambridge University Press.
- Pruppacher, H. R., J. D. Klett, and P. K. Wang (1998), *Microphysics of clouds and precipitation*, Taylor & Francis.
- Reade, W. C., and L. R. Collins (2000), Effect of preferential concentration on turbulent collision rates, *Phys. Fluids*, 12(10), 2530–2540.
- Saffman, P. G., and J. S. Turner (1956), On the collision of drops in turbulent clouds, *J. Fluid Mech.*, 1, 16–30.
- Sardina, G., F. Picano, L. Brandt, and R. Caballero (2015), Continuous growth of droplet size variance due to condensation in turbulent clouds, *Phys. Rev. Lett.*, 115(18), 184,501.
- Schiller, L., and A. Naumann (1933), Fundamental calculations in gravitational processing, *Zeitschrift des Vereines Deutscher Ingenieure*, 77, 318–320.
- Seinfeld, J. H., and S. N. Pandis (2016), *Atmospheric chemistry and physics: from air pollution to climate change*, John Wiley & Sons.
- Shaw, R. A. (2003), Particle-turbulence interactions in atmospheric clouds, *Annu. Rev. Fluid Mech.*, 35(1), 183–227.
- Shaw, R. A., W. C. Reade, L. R. Collins, and J. Verlinde (1998), Preferential concentration of cloud droplets by turbulence: Effects on the early evolution of cumulus cloud droplet spectra, *J. Atmosph. Sci.*, 55(11), 1965–1976.
- Shima, S., K. Kusano, A. Kawano, T. Sugiyama, and S. Kawahara (2009), The super-droplet method for the numerical simulation of clouds and precipitation: a particle-based and probabilistic microphysics model coupled with a non-hydrostatic model, *Quart. J. Roy. Met. Soc.*, 135, 1307–1320.
- Sundaram, S., and L. R. Collins (1997a), Collision statistics in an isotropic particle-laden turbulent suspension. part 1. direct numerical simulations, *J. Fluid Mech.*, 335, 75–109.
- Sundaram, S., and L. R. Collins (1997b), Collision statistics in an isotropic particle-laden turbulent suspension, *J. Fluid. Mech.*, 335, 75–109.

- Veysey, J., II, and N. Goldenfeld (2007), Simple viscous flows: From boundary layers to the renormalization group, *Reviews of Modern Physics*, 79(3), 883–927.
- Völk, H. J., F. C. Jones, G. E. Morfill, and S. Röser (1980), Collisions between grains in a turbulent gas, *A & A*, 85, 316.
- Voßkuhle, M., A. Pumir, E. Lévêque, and M. Wilkinson (2014), Prevalence of the sling effect for enhancing collision rates in turbulent suspensions, *J. Fluid Mech.*, 749, 841–852.
- Wang, L.-P., and W. W. Grabowski (2009), The role of air turbulence in warm rain initiation, *Atmosph. Sci. Lett.*, 10(1), 1–8.
- Wilkinson, M. (2016), Large deviation analysis of rapid onset of rain showers, *Phys. Rev. Lett.*, 116(1), 018,501.
- Wilkinson, M., B. Mehlig, and V. Bezuglyy (2006), Caustic activation of rain showers, *Phys. Rev. Lett.*, 97, 048,501.
- Zsom, A., and C. P. Dullemond (2008), A representative particle approach to coagulation and fragmentation of dust aggregates and fluid droplets, *Astron. Astrophys.*, 489(2), 931–941.